Probability and distribution of green water events and pressures

Boon, A.D.; Wellens, P.R.

DOI
10.1016/j.oceaneng.2022.112429

Publication date
2022

Document Version
Final published version

Published in
Ocean Engineering

Ocean Engineering 264 (2022) 112429

Contents lists available at ScienceDirect

Ocean Engineering

journal homepage: www.elsevier.com/locate/oceaneng

Probability and distribution of green water events and pressures

A.D. Boon, P.R. Wellens *

Faculty of Mechanical, Maritime and Materials Engineering, Delft University of Technology, 2628 CD Delft, The Netherlands

ARTICLE INFO

Keywords:
Green water
Large data set
Long-running experiments
Wave–current tank
Probability
Statistical distribution pressures

ABSTRACT

This article proposes a method to quantify, first, the probability of occurrence of green water and, second, the expected maximum pressures during green water events using their statistical distribution for ships at forward speed. A large green water data set which represents 1945 hours of continuous sailing on full scale with different sea states, forward speeds and drafts was obtained with model test experiments in a wave–current tank. The data of the experiment are available as open data through https://doi.org/10.4121/21031981. With the large data set obtained, the distribution of the time between green water occurrences is identified as exponential, indicating that when green water occurs is independent of the time since the last occurrence. Two methods were compared to estimate the probability of green water occurrence. One method is based on the probability of water exceeding the deck and one on a ship's freeboard and the significant wave height, the former being in better agreement with the data, the latter being more practical for designers. The maximum pressures caused by green water are distributed according to the Fréchet distribution, also called extreme value distribution II. With the newly identified distributions, finally, an equation to calculate the probability of a pressure limit being exceeded for a ship in operation is formulated.

1. Introduction

Ships are out in the ocean to transport the many goods we send around the world, to provide protection, or to place wind turbines, among other activities. Waves interact with these ships, sometimes in ways that lead to impacts. Green water is one of these impact types. Green water is water that crashes on the deck or against superstructures and can lead to large impact pressures. They are extreme events, which means that they do not occur often. But when they occur they can cause damage. As Buchner (2002) stated, green water is a nonlinear and strongly complex problem.

Knowing how often these green water events occur during a ship's lifetime is helpful for ship design. In literature, the probability of water exceeding the deck or deck wetness has been used as an analogy for the probability of green water. The exceedance probability is often obtained from setups with mainly fixed, ship-like models in irregular waves (Buchner, 2002; Ogawa, 2003; Guedes Soares and Pascoal, 2005). Probabilities of exceedance have also been found based on simplified setups with a static box above water without forward speed (Cox and Scott, 2001; Mori and Cox, 2003). All these methods depend on the probability of a wave exceeding the deck, while Greco (2001) found green water events where deck exceedance did not occur prior to green water: hammer-fist type events. On the other hand, exceedance events are not always green water events, as white water and spray events also occur, but do not induce the large pressures and subsequent damage (Greco et al., 2007). The probability of green water occurrence, in the strict definition that it needs to lead to large pressures, has, to the authors' knowledge, not yet been quantified.

Then, besides the occurrence of green water, also the expected pressures caused by green water events are needed to design for green water. For the pressures much research focuses on the pressure and pressure development during an event, using static box shapes in regular or breaking waves (Hernández-Fontes et al., 2020a,b; Song et al., 2015; Ariyarathne et al., 2012; Lee et al., 2012; Faltinsen et al., 2002; Mori and Cox, 2003). From a design perspective, however, also the distribution of the maximum pressures over a range of green water events is of interest as this would give the expected pressures on a ship during a green water event. Hamoudi and Varyani (1998) give significant loads for a sailing ship model in irregular waves but do not show the distribution or other statistics. Ogawa (2003) gives a calculation method to find the probability of a mean deck load being exceeded using a relation between exceedance level and load. The resulting method is based on the probability density function of the relative water height, not the actual distribution of the loads. Guedes Soares and Pascoal (2005) fitted a distribution to the water height maxima, which is related to pressures (Buchner, 2002; Ogawa, 2003), but stated that more work is needed. Research by Fonseca and Guedes Soares (2005) gives the pressures on a ship model in large irregular waves but

* Corresponding author.
E-mail address: p.r.wellens@tudelft.nl (P.R. Wellens).

https://doi.org/10.1016/j.oceaneng.2022.112429
Received 30 June 2022; Received in revised form 25 August 2022; Accepted 26 August 2022
Available online 27 September 2022

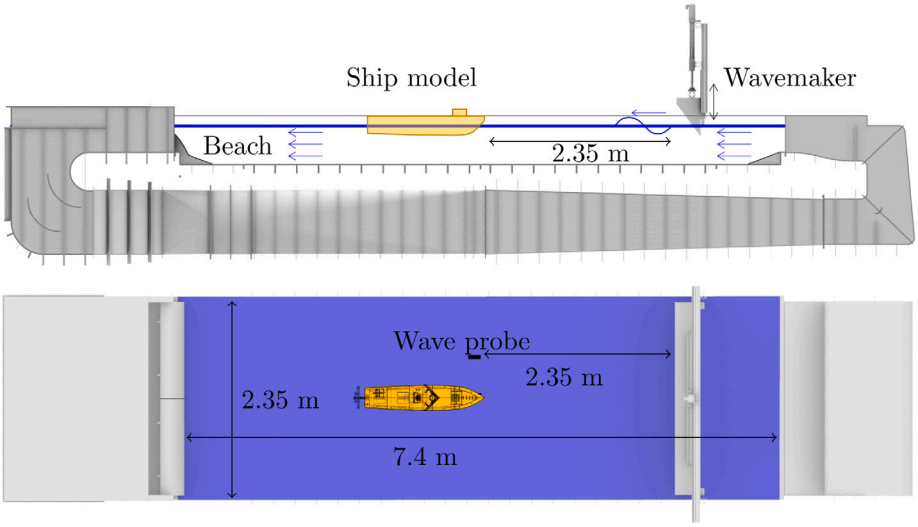

Fig. 1. Side and top view of the new wave–current tank used for the long-running continuous experiments.

concludes that due to the limited amount of data no definitive relations could be derived. A statistical investigation with a large data set of pressures on deck thus remains to be performed. Specifically, a large data set of green water events on a sailing ship with forward speed in irregular waves is needed to find the actual statistical distribution of the pressures induced by green water events for a ship in operation.

The main objective of this article is therefore to propose a method to quantify, first, the probability of occurrence of green water with significant pressures and, second, the expected maximum pressures during a ship's lifetime by finding the pressures' probability distribution. For this a large amount of green water events on a ship in realistic sailing conditions is needed. Because green water events are rare in realistic sailing conditions, obtaining such a data set is challenging as large testing times are required. Towing tanks used normally have limited length, and thus limited testing time when including forward speed. To get around these limitations, we have conducted experiments in an existing free surface current tank, that was extended with a new wave maker and wave spending beach for the purpose of this study. In this wave–current tank, the model is kept stationary while the water flows, removing the time limitation and allowing for 40-hour long sea states at forward speed. This article describes the experimental setup, the data collection and processing, the fitting of distributions, estimation methods for the probability of green water occurrence, and how to determine the probability of a limit pressure being exceeded during the life time of a ship with a method beneficial for design purposes. The data of the experiments have been shared as open data through the 4TU.ResearchData repository (Wellens and Boon, 2022)

2. Experiments

A large amount of green water data was collected to find the probability of green water occurrence and statistical distributions of the pressure following green water events. The experiments model a ship in irregular waves, with free heave and pitch, forward speed and different sea states. Head waves are used as they lead to the most severe green water impacts (Berhault and Guerin, 1998). The data set includes the occurrence of green water, as well as the pressures during the green water events on the deck and deck box that models a structure.

2.1. Test facility

A new facility is constructed for this research by adding a wavemaker and spending beach to the existing current tank at Delft University of Technology. In doing so a wave–current tank was created in which a ship model is stationary while the water and waves flow past it, enabling 40-hour long sea states with modelled forward speed. The wave–current tank has a test section with a length of 7.4 m, a width of 2.35 m and a used water depth of 0.435 m. A schematic of the tank is shown in Fig. 1. A turbine in the bottom part of the tank creates a current. By adjusting the frequency of the wedge-shaped plunging type wavemaker as shown in Lowell and Irani (2020), the generated waves were such as to model a sea state through which the model sails with a forward speed V, which is equal to the current velocity in the tank. To minimize reflections a parabolic-shaped stainless steel mesh beach was designed and placed at the end of the test section. A test campaign with regular waves was carried out before the actual experiments to find the transfer functions of the wavemaker, which was necessary because of the interaction between the wavemaker and current.

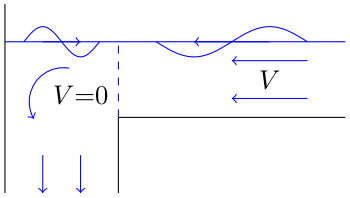

Fig. 2. Area at the outflow of the wave–current tank (left side Fig. 1) that influences the reflection coefficients. Horizontal velocity indicated as V.

2.1.1. Reflection of the waves

The test campaign also verified that reflected waves did not interfere with the conducted experiments. The incident and reflected wave amplitude were measured separately by using regular wave trains of a time length shorter than the time it takes the first wave to travel from the wavemaker to the beach and back to the wave probe. The reflection coefficient is defined as the reflected wave amplitude divided by the incident wave amplitude of those measurements. The tests were repeated for various flow velocities, wave periods and amplitudes. A maximum reflection coefficient of 0.08 at current velocities of 0.21 m/s and wave frequencies of 5 rad/s was found. The reflection coefficient decreases quickly to 0 for larger current velocities and higher wave frequencies. The reflection coefficient is mainly affected by the spending beach, but also by the configuration behind the beach. The configuration of the tank behind the beach features a complex interaction between wave components and the apparent water depth changes together with the change in direction of the flow. This is shown in Fig. 2. The interaction is beneficial for low reflection coefficients.

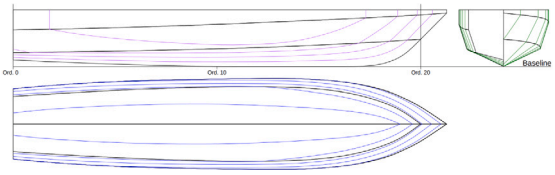

Fig. 3. Lines plan of the used ship model.

Table 1
Dimensions and parameters of the used model.

Parameters	Values
Length between perpendiculars	1.50 m
Breadth moulded	0.330 m
Depth moulded	0.207 m
Draft	0.105/0.117/0.126 m
Total mass	41.0/46.0/51.0 kg
Vertical centre of gravity	0.161 m
Longitudinal centre of gravity	0.703 m
Radius of gyration in pitch	0.366 m
Natural heave frequency	1.12/1.11/1.10 Hz
Natural pitch frequency	1.64/1.64/1.64 Hz
Deck box (L × W × H)	0.150 × 0.180 × 0.090 m
Distance to deck box from stem	0.300 m
Location RWE probe from stem	0.04 m

2.2. Ship model

The ship model is placed in the middle of the wave–current tank as shown in Fig. 7, with 2.35 m between the front of the wavemaker and the stem of the model. A yaw limiter and heave rod were used to mount the ship, leaving only heave and pitch as free motions.

The ship model is no. 523 from the Delft Systematic Deadrise Series. The lines plan is shown in Fig. 3. The model is a planing hull model which in the experiments is used as a displacement hull. It has a basic ship-like shape with a flat aft and a tapered bow. In Table 1 the dimensions of the model are shown. A deck box with the dimensions shown in Table 1 is placed on deck to represent a deck structure. Swing tests were done to find the radius of gyration. The shown draft (D) was found by measuring the freeboard at the location of the relative water elevation (RWE) probe using a measuring tape. To get different drafts of the vessel, weights were placed on top of the heave rod. For the different drafts, the natural heave and pitch frequencies were obtained with excitation tests.

2.3. Test conditions

Eleven long-running tests were conducted with 174 hours of testing time in total. Different wave spectra, modelled forward velocities and drafts were tested.

Statistically representative sea states were generated by creating 40-hour long wave files with a high frequency resolution below 0.05 mHz. Wave spectra with different energy distributions were created, as the measured spectra translated to an earth-fixed frame in Fig. 4 show. The transfer function between wavemaker and wave changed for different modelled forward speeds. Thus the spectra tested for different modelled forward velocities were similar but not identical, as shown in Fig. 5.

Properties of conducted tests are shown in Table 2. Here, T_p is the peak frequency in the earth-fixed frame of reference, H_{m0} the spectral significant wave height, T_{z_e} the zero-crossing encounter period of the spectra, which depends on V. The experiments continued for different testing durations, indicated with t_{test}. n_{GW} is the number of green water events that occurred during a test and P_{GW} is the probability of green water per encountered wave. The number of encountered waves (n_w) was estimated with T_{z_e} and t_{test}.

With the chosen test conditions limitations are introduced. The tested wave spectra are all within a limited range of peak periods

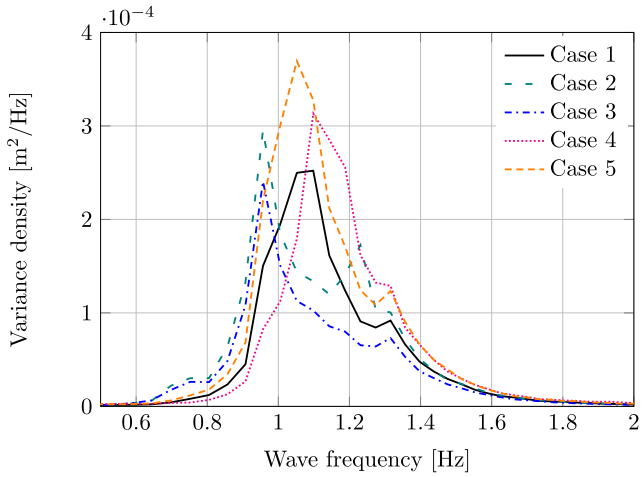

Fig. 4. Wave spectra for earth-fixed frame of reference with different energy distributions for experiments with a modelled forward speed of 0.25 m/s.

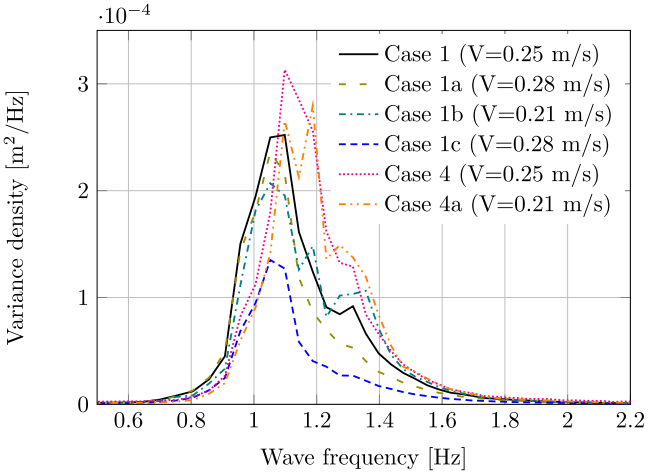

Fig. 5. Wave spectra for earth-fixed frame of reference with two types of energy distributions for experiments with different modelled forward speeds and a draft of 0.117 m.

and significant wave heights, which will limit the applicability of the results. More tests need to be conducted in future. The applicability of the results is also limited to ships that are sufficiently similar to the used ship model. As the wave spectra tested for different modelled forward velocities are similar but not identical, it is not possible to investigate the effect of forward velocity on pressures as an independent variable.

2.3.1. Full scale comparison

To confirm that the numbers in Table 2 model realistic situations, a Froude scaling factor of 125 is assumed based on the ship model likeness to naval vessels of about 190 m long like the Austin-class, but without a bulb (Federation of American Scientists, 1999). The total testing time shown in Table 2 would translate to about 1945 continuous sailing hours. According to the scaling factor of 125, the water depth is 54 m, the peak periods vary between 9.2 and 11.7 s and the significant wave heights between 3 and 5.3 m. These are rough (5) to very rough (6) sea states according to the Douglas sea scale. These sea states cover a small but relevant part of the scatter diagram of possible sea states. The sailing speed is between 4.6 and 6.1 knots, which is low but representative of a ship sailing through rough seas. Using scaled experiments introduces limits in the applicability of the pressure results since density, viscosity and surface tension are not accounted for when

Table 2
Test cases.

Case	T_p [s]	H_{m0} [m]	T_{z_c} [s]	V [m/s]	D [m]	t_{test} [h]	n_{GW}	P_{GW}
1	0.95	0.035	0.67	0.25	0.117	8	9	0.00021
1a	0.97	0.034	0.67	0.28	0.117	8	7	0.00016
1b	0.93	0.038	0.65	0.21	0.117	8	20	0.00045
1c	0.97	0.024	0.67	0.28	0.117	8	0	0
2	1.05	0.032	0.68	0.25	0.117	40	2	0.00001
3	1.05	0.038	0.68	0.25	0.117	40	34	0.00016
4	0.91	0.040	0.61	0.25	0.117	40	199	0.00084
4a	0.82	0.042	0.62	0.21	0.117	2	9	0.00083
5	0.95	0.042	0.67	0.25	0.117	14	91	0.00119
4 D_+	0.91	0.040	0.61	0.25	0.105	3	6	0.00034
4 D_-	0.91	0.040	0.61	0.25	0.126	3	32	0.00181
Total						174	409	

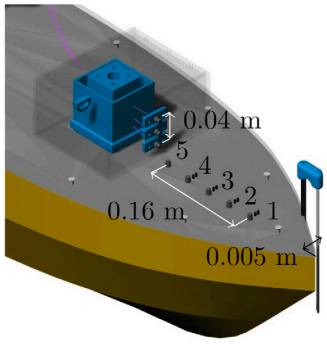

Fig. 6. Bow of the ship model with locations of sensors. The pressure sensors are on the starboard side and the wetness sensors are on the port side of the ship model.

using Froude scaling (Song et al., 2015). A scaling factor of 125 is in line with scaling factors in other green water research with values of 100 (Ruggeri et al., 2015; Song et al., 2015; Lee et al., 2012), 125 (Abdussamie et al., 2017; Lee et al., 2020) and 169 (Ariyarathne et al., 2012).

2.4. Data acquisition

To measure the impacts of interest on the deck and deck box, five pressure sensors were placed on the deck and three on the deck box as shown in Fig. 6. The pressure sensors are GE druck PDCR 42 type sensors with a range up to 350 kPa. Two deck pressure sensors, number 2 and 5 in Fig. 6, broke during the experiments and their data was not used. The net frequency of 50 Hz induced noise into the pressure signal so the signal was filtered with a 2nd order low pass filter at 45 Hz. To be able to identify when an event occurred, wetness sensors were placed next to the front four deck pressure sensors. The wetness sensors consist of small probes on deck measuring changes in the electrical resistance, giving as a result of their limited height a binary wet or not signal. The motions of the vessel were measured using Panasonic HG-C1400 laser distance sensors. One was placed next to the hinge in the centre of gravity to measure heave, and the second 0.682 m from the first to the aft of the vessel to measure pitch. A load cell was placed in the hinge to measure overall resistance, as well as in the deck box to measure the force of a large impact. The overall setup is shown in Fig. 7. A resistance type wave probe was placed 1.15 m port of the vessel, and 0.64 m from the side of the tank. The wave probe was at the same location in the lengthwise direction of the tank as the resistance type RWE probe at 2.35 m from the closest point of the wavemaker. The RWE probe was attached at the port side of the bow of the model 0.05 m from the centre and 0.04 m behind the stem. Appendix A gives an uncertainty analysis based on the measurement errors.

The experiments were automated to allow them to be long-running and continuous for up to 40 hours. To allow for the large amounts of data to also automatically be saved a new data acquisition system was needed. Two DAQ devices (NI 6009 and NI 6211) were used to control the wavemaker and save data. The data sampling rate was 1000 Hz as peak pressures act for times of about 1 millisecond (Peregrine, 2003). A LabVIEW programme was made to synchronize and save the data to separate TDMS files, each containing 20 minutes' worth of data. The files were automatically backed up during the experiments to an offsite location to prevent data loss.

As the experiments were automated, no live in-person supervision of the data was performed. A system was set up using www.twitch.tv, normally used for live streaming video games, which allowed for live offsite supervision and which automatically saved all footage for later review. Footage of both the top and the side of the bow of the vessel was taken in sync at 30 Hz. Images of the footage during a green water event are shown in Fig. 8.

2.5. Event identification

Green water events are identified using wetness sensors and visual identification. Green water events in the present study are defined as a flow of water on deck that reaches at least the most forward wetness or pressure sensor, located 0.012 m behind the stem of the bow. This definition only excludes spray-like events, which induce pressures lower than the pressure found during green water events. The data and visual footage of each event were checked to ensure the quality of the data. Pressure sensor data from one event from case 4 was deemed unusable due to an impact event against the tank during the event which induced noise in all the pressure sensors.

Most events did not reach the deck box. Events that did reach the box are sorted based on the maximum pressure found on the box. 41 events were included in the deck box impact data set.

Exceedance events are defined as the RWE probe measuring a water level above deck height for at least 0.01 s.

3. Results

Before analysing the results, their relation to results from previous research is found. Both the pressure and the impact durations are considered and compared to results from Ariyarathne et al. (2012), Hernández-Fontes et al. (2021), Cuomo et al. (2010), Hattori et al. (1994) and Song et al. (2015).

The relation between rise time of the pressure (t_r) and maximum pressure on deck ($p_{max,deck}$) is known to be $p_{max,deck} = a{t_r}^b$. Fig. 9 shows a pressure trace with t_r and t_d indicated, which were calculated with the zero-crossing times before and after the peak and the time at which the peak value was measured. Fig. 10 shows for one impact from each tested case the pressure time traces of the deck pressure sensors. The coefficients a and b have been empirically determined for coastal structures (Hattori et al., 1994; Cuomo et al., 2010; Kirkgoz, 1990) and green water on ships (Song et al., 2015; Ariyarathne et al., 2012). For the present study the relation between t_r and $p_{max,deck}$ is

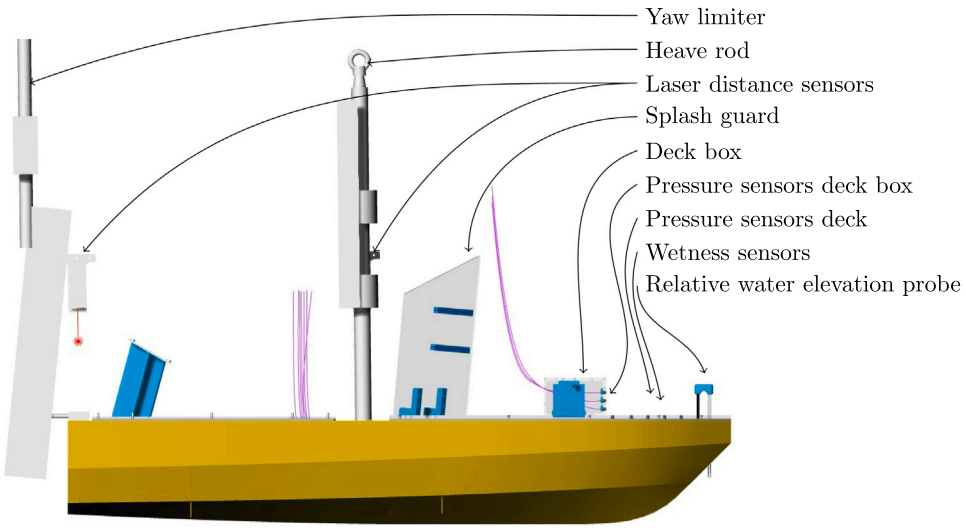

Fig. 7. Side view of test setup.

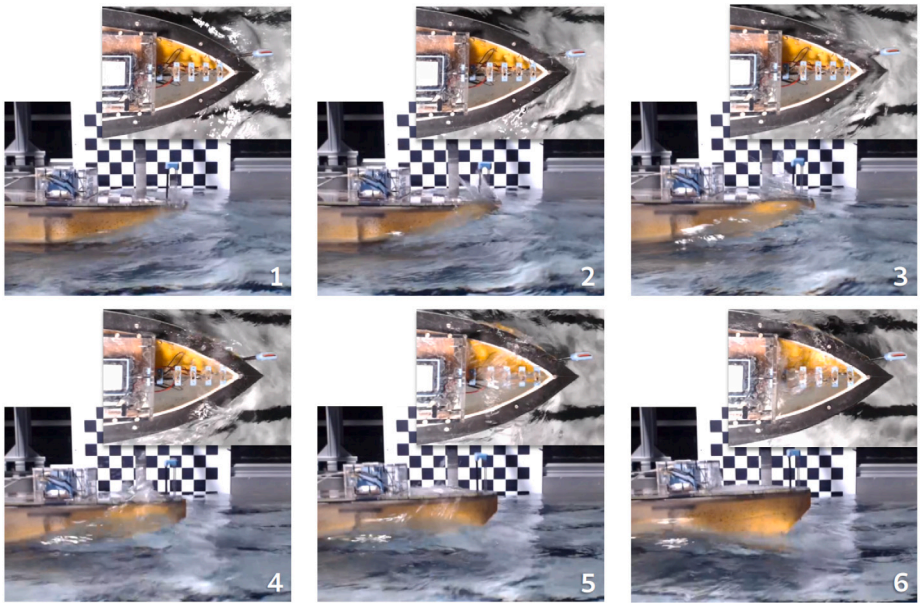

Fig. 8. Example of video footage to monitor the long-running experiments. Images numbered 1 to 6 in chronological order showing a 0.2 s period with a green water event.

shown in Fig. 11. The spread in the figure is similar to the spread in the figures found in Cuomo et al. (2010), Hattori et al. (1994) and Song et al. (2015). The parameters for the best fit with b limited to values found in literature are $a = 17.3$ and $b = -0.6$. Note that the parameters are dimensional thus scale will influence the results. The fits from Song et al. (2015) and Ariyarathne et al. (2012) with scaling factors of 100 and 169 are shown.

Second, the pressure development quantified by the relation between t_r and impact duration t_d is compared. Previous research considered consecutive green water events on a fixed structure, caused by regular waves finds for t_r/t_d a spread of data between 0.18 and 0.64 over 120 events (Hernández-Fontes et al., 2021). The range of t_r/t_d found in the present study is shown in Fig. 12. Our research considers a larger range, with most events within the expected 0.18 to 0.64 range. Events in the present study were smaller, with smaller peak pressures, compared to the events in Hernández-Fontes et al. (2021), leading to a smaller t_r/t_d because of the inverse relationship between the rise time and pressure peak. The larger values in the present study for t_r/t_d found might not be a result of the physics of the impact but caused by water

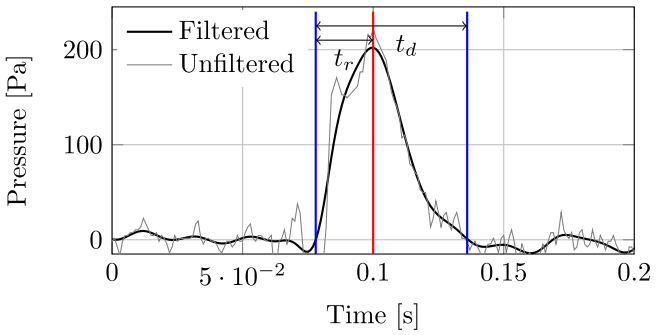

Fig. 9. Pressure trace of green water event on pressure sensor 1 in case 4 with rise time t_r and duration time t_d indicated.

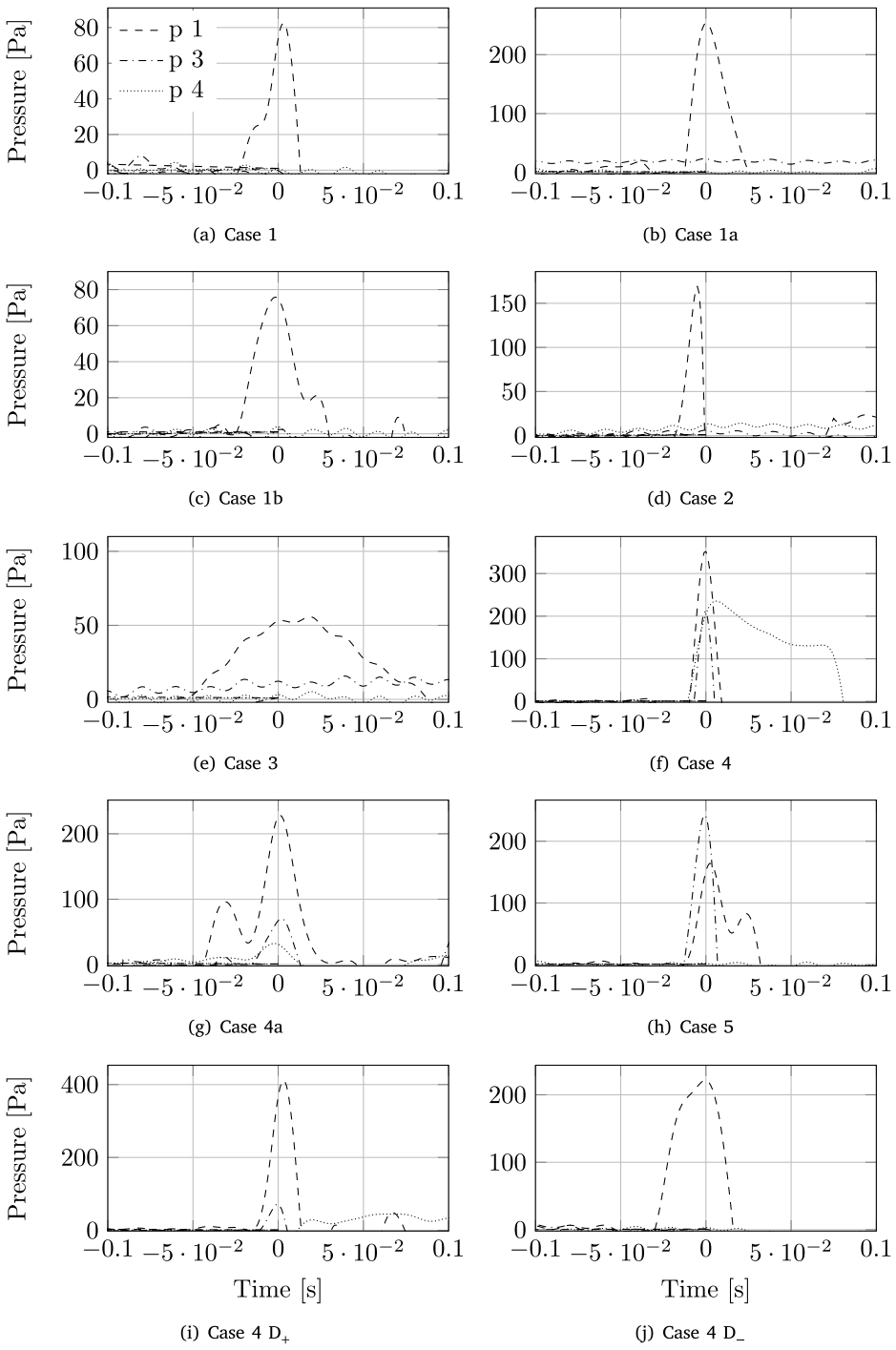

Fig. 10. Pressure signals on deck pressure sensors for one event from each test case. The data is time-shifted so the pressure peak occurs at 0 for each sensor.

on the pressures sensor cooling the sensor, causing a faster decrease in measured pressures, leading to a lower value of t_d. Overall the shown data agrees with the spread found by Hernández-Fontes et al. (2021).

Summarizing, the data from the present study is in accordance with previous research, with a larger spread in events and number of events. More low pressures, indicating lower fluid velocities, are present in the data set in the present study. Previous research focused on the physics or categorization of individual green water events, for which a large enough impact is necessary for analysis. This goal is in contrast with the present study which focuses on the distribution of all sizes of green water impacts.

3.1. Distributions of event occurrence

The distribution of the occurrence of green water events over time has been identified for each tested case with more than 10 green water events, which were cases 1b, 3, 4, 4 D_ and 5. The time between the occurrence of green water events is used to base distributions on. For each case distributions are fitted through the set of times between events. The distributions were the Gumbel, Fréchet, Weibull, chi, chi-squared, Rayleigh, Cauchy, exponential, exponential power, power law, gamma, normal, log-normal, and uniform distribution. By using the least-squares method on the data in 100 bins the best fit is found for each case.

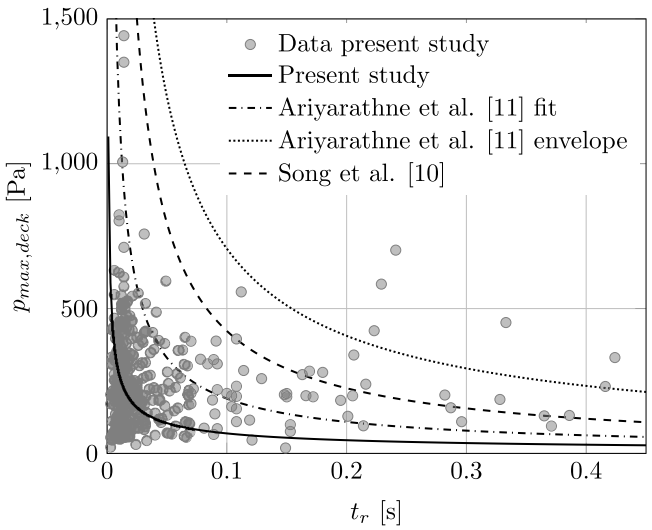

Fig. 11. Relation t_r and $p_{max,deck}$ with best fit and previous found correlations shown, the results from the present study show lower rise times compared to previous research.

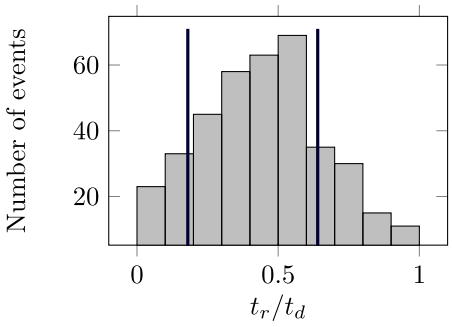

Fig. 12. Histogram of t_r/t_d showing overall agreement with $0.18 < \frac{t_r}{t_d} < 0.64$ found by Hernández-Fontes et al. (2021). A larger range of impacts is found for the present study.

The best-fitting distribution for the times between events was overall the exponential distribution. For some cases the gamma distribution gave a better fit, but this was for cases with fewer events. The exponential distribution is a special case of the gamma distribution and has one free parameter fewer to fit with compared to the gamma distribution. The extra parameter means that for data with more variance than the sample mean (as is the case for smaller data sets) the gamma distribution has an extra parameter to force a better fit. The time between events is concluded to be exponentially distributed.

The exponential distribution is in line with green water events occurring continuously and independently at a constant average rate. Thus, the time when a green water event occurs is independent of the time since the last event. The results of the distribution for case 4, the case with the most green water events, are shown in Fig. 13(a) with the experimental data visualized in 35 bins. A quantile–quantile plot (Q–Q plot) for case 4 is shown in Fig. 13(b). The Q–Q plot visualizes outliers and overall deviations from the distribution with a diagonal line indicating a perfect fit (Wilk and Gnanadesikan, 1968). The plot shows some outliers but a general agreement with the distribution. This is the conclusion for other cases as well.

For further verification, an exponential distribution was fitted for all the cases. The parameters of the fitted exponential distributions are shown in Table 3. In this table, λ is the mean time between events.

A goodness-of-fit test was conducted for the fitted distributions using the Kolmogorov–Smirnov (KS) test. The test uses the maximum difference between an empirical and hypothetical cumulative distribution and gives a p-value (Massey, 1951). A limit of 0.05 is set for the p-value, meaning that for p-values below 0.05, the distribution is concluded to not represent the data. The results for the goodness-of-fit test are shown in Table 3. All p-values are well above 0.05. The exponential fit can thus represent the empirical data of the time between green water events.

Besides the green water events also the distribution for the time between exceedance events is identified and is also found to be exponentially distributed. The results of the fit and the KS goodness-of-fit test are also shown in Table 3. As again all values are above 0.05 the exponential fit is also a suitable distribution for the distribution of the time between exceedance events.

3.2. Distributions of pressures

To analyse the pressures on the deck and deck box the measured pressures are captured in parameters $p_{deck,max}$, $p_{box,max}$, $P_{deck,max}$ and $P_{box,max}$. The local maximum pressure on deck $p_{deck,max}$ is the maximum pressure measured by one of the sensors during a green water event. The maximum local pressure on the deck box is $p_{box,max}$. The mean maximum pressure $P_{deck,max}$ is the maximum pressure measured per event per deck sensor, averaged over all the deck sensors. $P_{box,max}$ is the mean maximum pressure on the deck box.

The pressures are thought to depend on the sea state, as Guedes Soares and Pascoal (2005) found larger mean relative water height maxima for larger H_{m0}. As the relative water heights are known to relate to the maximum pressure (Buchner, 2002; Ogawa, 2003), different pressures are expected for different cases. Cases 4 and 5, with more than 50 green water events each, are used for further statistical analysis.

The same method is used to find the distributions of pressures as is used to find the distribution of occurrence of events in paragraph 3.1. With this method, the sum least-square error applied over the data binned in 100 bins showed the Fréchet distribution, also known as the inverse Weibull distribution, to be the best fit. Fig. 14, for case 4, shows the fit and the experimental data visualized in 35 bins. When one takes the maximum of a set of variables, which is done for $p_{deck,max}$ and $p_{box,max}$, the distribution of the overall data will always become an extreme value distribution (de Haan and Ferreira, 2000). This fact is in line with the Fréchet distribution fitting the results as the Fréchet distribution is the generalized extreme value distribution type II.

The pressures on both the deck and deck box for both cases 4 and 5 are concluded to be distributed according to the Fréchet distribution. To further the confidence in the fit of the Fréchet distribution again the KS goodness-of-fit test was conducted. The results are shown in Table 4. All p-values are larger than the acceptance limit of 0.05, also when fitting a Fréchet distribution for $P_{deck,max}$ and $p_{deck,max}$ for the other cases than 4 and 5 with more than 10 green water events. The size of the deck box data set is considered too limited, as discussed in paragraph 2.5, consisting of 23 events for case 4 and of 9 events for case 5. The skewness of the pressures on the deck box is therefore not reported in Table 4 (dashes are shown instead) and the deck box pressures are not included in further analysis.

The highest pressures that occur are of most interest from an engineering perspective as they cause the largest damages. The representation of those highest pressures by the fitted distribution is thus investigated. To visually inspect how well the Fréchet distribution fits the extreme cases, Q–Q plots are shown in Fig. 15. For case 4 the fitted distribution overestimates the larger pressures for both $P_{deck,max}$ and $p_{deck,max}$. For case 5 the two highest values for $p_{deck,max}$ deviate from the distribution, causing the largest $P_{deck,max}$ to also deviate from the distribution. The deviation from the distribution further away from the mean of the distribution can be quantified using the skewness (s). Higher values of skewness indicate more values further away from the mean. The values for the skewness are shown in Table 4. All values

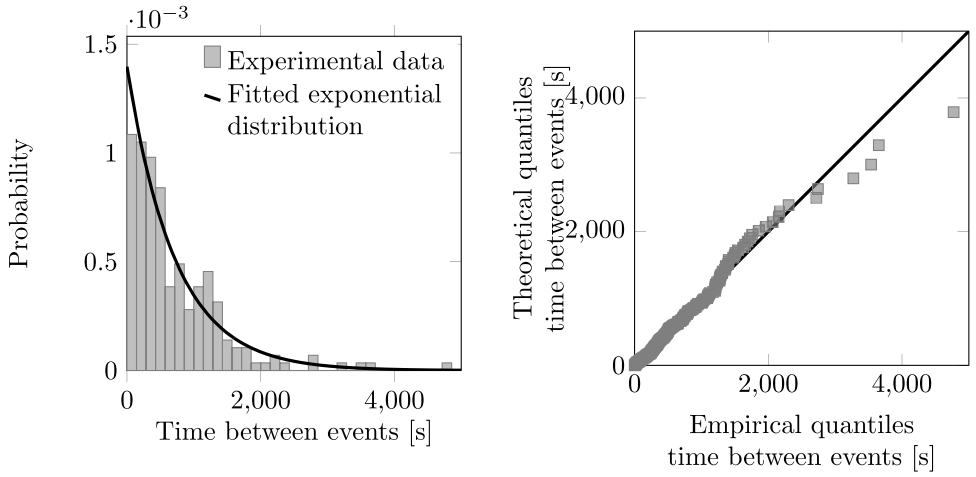

(a) Histogram of experimental data and the fitted exponential distribution

(b) Q-Q plot showing the distribution fits the data well

Fig. 13. Time between green water events for case 4 and the fitted exponential distribution.

Table 3
Parameters of fitted exponential distribution for time between green water and exceedance events and p-values from Kolmogorov–Smirnov goodness-of-fit test.

Case	Green water occurrence			Deck exceedance occurrence		
	Parameters [s]		p-value	Parameters [s]		p-value
	Location	λ_{GW}		Location	λ_{EX}	
1	162	3200	0.76	129	1065	0.69
1a	286	4114	0.37	34.6	2119	0.64
1b	151	1440	0.77	2.26	710	0.12
1c	–	–	–	–	–	–
2	1857	72000	0.50	1402	48000	0.12
3	64.0	4235	0.88	63.2	2321	0.65
4	1.00	724	0.48	1.45	439	0.26
4a	182	732	0.93	2.90	210	0.51
5	3.00	564	0.50	1.41	296	0.41
4 D_+	185	1800	0.74	3.58	477	0.73
4 D_-	6.00	338	0.74	1.43	171	0.59

Table 4
Parameters of fitted Fréchet distribution, p-value from Kolmogorov–Smirnov test and skewness of data and distribution for $p_{deck,max}$, $p_{box,max}$, $P_{deck,max}$ and $P_{box,max}$.

Case 4	Parameters			KS-test	Skewness	
	Shape	Location	Scale	p-value	s_{data}	s_{distr}
$p_{deck,max}$	6.57	−511	663	0.361	0.427	11.6
$p_{box,max}$	0.417	31.2	11.5	0.066	–	–
$P_{deck,max}$	3.40	−84.5	164	0.059	0.496	2.56
$P_{box,max}$	0.503	18.5	7.15	0.159	–	–
Case 5	Shape	Location	Scale	p-value	s_{data}	s_{distr}
$p_{deck,max}$	8.06	−243	447	0.062	0.881	2.18
$p_{box,max}$	0.496	30.9	6.34	0.888	–	–
$P_{deck,max}$	10.1	−264	371	0.440	0.670	1.90
$P_{box,max}$	0.531	20.2	2.13	0.961	–	–

show a skewness larger than 0, indicating a skew to values above the mean. The skew of the theoretical distribution is for both cases for both $p_{deck,max}$ and $P_{deck,max}$ larger than the skew of the empirical data. The fitted Fréchet distribution thus estimates more pressure above the mean pressure compared to the number of measured values, meaning that the Fréchet distribution gives a conservative estimation for pressures above the mean pressure.

3.3. Calculating probability pressure exceedance

In the previous paragraphs, first, the probability of green water occurring and second the distributions of the pressures are obtained. Now the probability that an event occurs during a ship's operation is calculated as

$$P_{GW} = \frac{n_{GW}}{n_w} = \frac{\frac{t}{\lambda_{GW}}}{\frac{t}{T_{z_e}}} = \frac{T_{z_e}}{\lambda_{GW}}. \tag{1}$$

In this equation, n_w is the number of waves encountered during a ship's operation. With the newly found distribution of the pressures, the probability of a certain limit pressure (p_{lim}) being exceeded during an event can be calculated with the cumulative distribution function of the Fréchet distribution

$$Pr(p_{deck,max} > p_{lim}) = 1 - exp(-\frac{p_{lim} - m}{c})^{\alpha}, \tag{2}$$

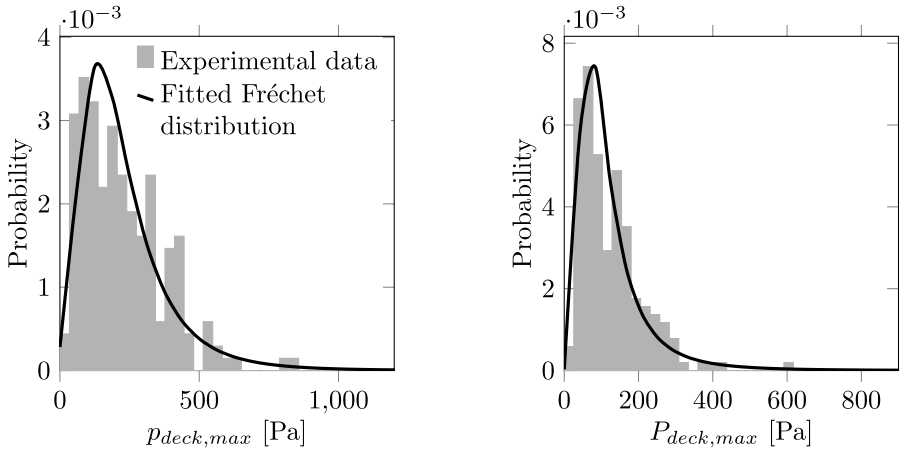

(a) $p_{deck,max}$ and the fitted Fréchet distribution

(b) $P_{deck,max}$ and the fitted Fréchet distribution

Fig. 14. Histograms of experimental data of case 4 with the fitted Fréchet distribution.

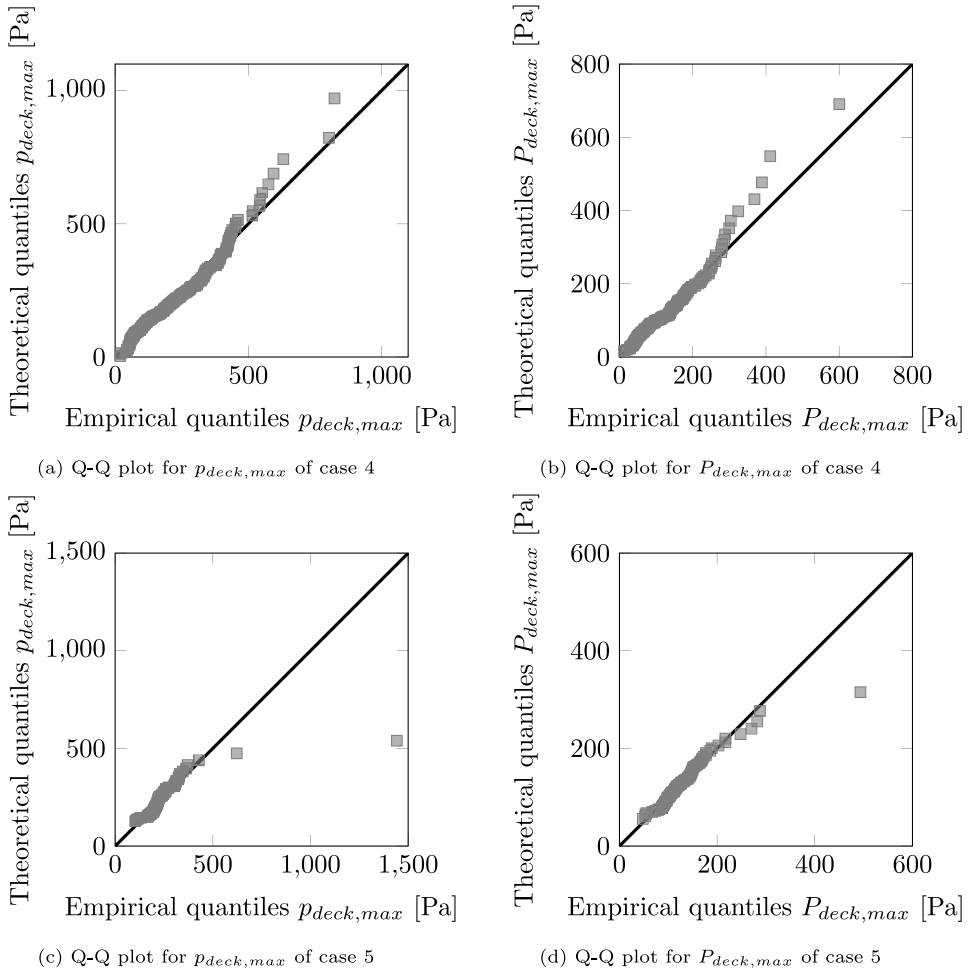

(a) Q-Q plot for $p_{deck,max}$ of case 4

(b) Q-Q plot for $P_{deck,max}$ of case 4

(c) Q-Q plot for $p_{deck,max}$ of case 5

(d) Q-Q plot for $P_{deck,max}$ of case 5

Fig. 15. Q–Q plots showing the quality of fit of the Fréchet to $P_{deck,max}$ and $p_{deck,max}$ for cases 4 and 5. The lines indicate the fitted theoretical distribution and the squares the experimental data.

in which m is the location parameter, c the shape parameter and α the scale parameter. The empirically found values for these parameters are given in Table 4.

Combining equation (1) and (2) and using compound probability theory gives us

$$\begin{aligned} Pr(p > p_{lim}) &= 1 - (1 - Pr(p_{deck,max} > p_{lim}))^{n_{GW}} \\ &= 1 - (exp(-\frac{p_{lim} - m}{c})^{\alpha})^{\frac{t}{\lambda_{GW}}}. \end{aligned} \tag{3}$$

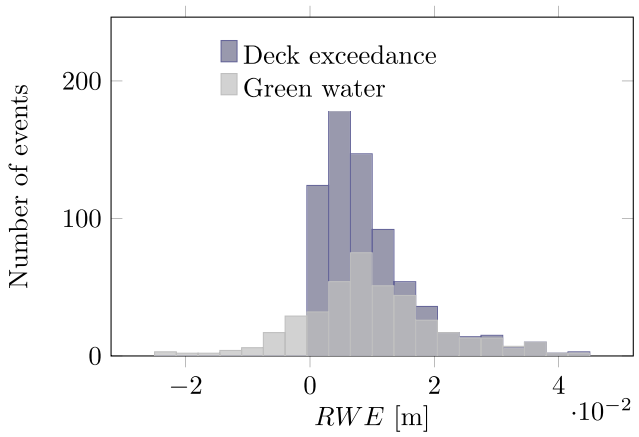

Fig. 16. Difference between green water events and deck exceedance events shown using the relative water elevation.

This equation gives the probability of a pressure on deck being exceeded during a ship's operation. As we will see below, the probability of green water occurring depends mostly on the sea state, draft and forward speed. For the pressure distribution a dependency on the sea state is known (paragraph 3.2).

The probability of a limit pressure being exceeded for a certain sailing time, sea state, draft and forward speed can now be calculated with Eq. (3). Note that the average probability of green water occurrence (λ_{GW} or P_{GW}) is independent of the distribution.

As the Fréchet distribution is conservative for the large pressures (paragraph 3.2), the probability calculated with Eq. (3) is also conservative for large pressures. This is assuming that the probability of green water occurrence is accurately or conservatively estimated.

3.3.1. Relation between the probability of green water and exceedance

In our experiments deck exceedance is not always measured when green water events occur, and exceedance does not always lead to green water, see Fig. 16. The figure shows green water occurring for relative water elevations lower than the deck, which is possible as some green water impact types like hammer-fist events occur when the measured freeboard is positive (Greco, 2001). Also, Fig. 16 shows that not all exceedances lead to green water, as is the case for exceedances below 0.015 m. This does not mean that for those exceedances no water comes on deck, as deck wetness with small amounts of water can still occur in the form of, for instance, spray, but this deck wetness does not meet the definition of green water used in this study (paragraph 2.5).

A relation between P_{GW} and the probability of an exceedance event occurring (P_{EX}) is valuable as P_{EX} is easier to obtain compared to P_{GW}, with various methods to estimate P_{EX} available in literature (Buchner, 2002; Cox and Scott, 2001; Ogawa, 2003; Guedes Soares and Pascoal, 2005; Hamoudi and Varyani, 1998). P_{EX} is calculated by dividing the number of individual exceedance events measured with the RWE probe by n_w. The average time between exceedance and green water events per case is given in Table 3. The relation between P_{EX} and P_{GW} is shown in Fig. 17. The dotted lines in the figure indicate the 95% confidence interval. The 95% confidence interval is approximated based on the exponential distribution of the events over time using the method described by Ross (2020), which underestimates the confidence interval for fewer than 15 events (Guerriero, 2012). The confidence interval depends on the number of events, which explains the differences.

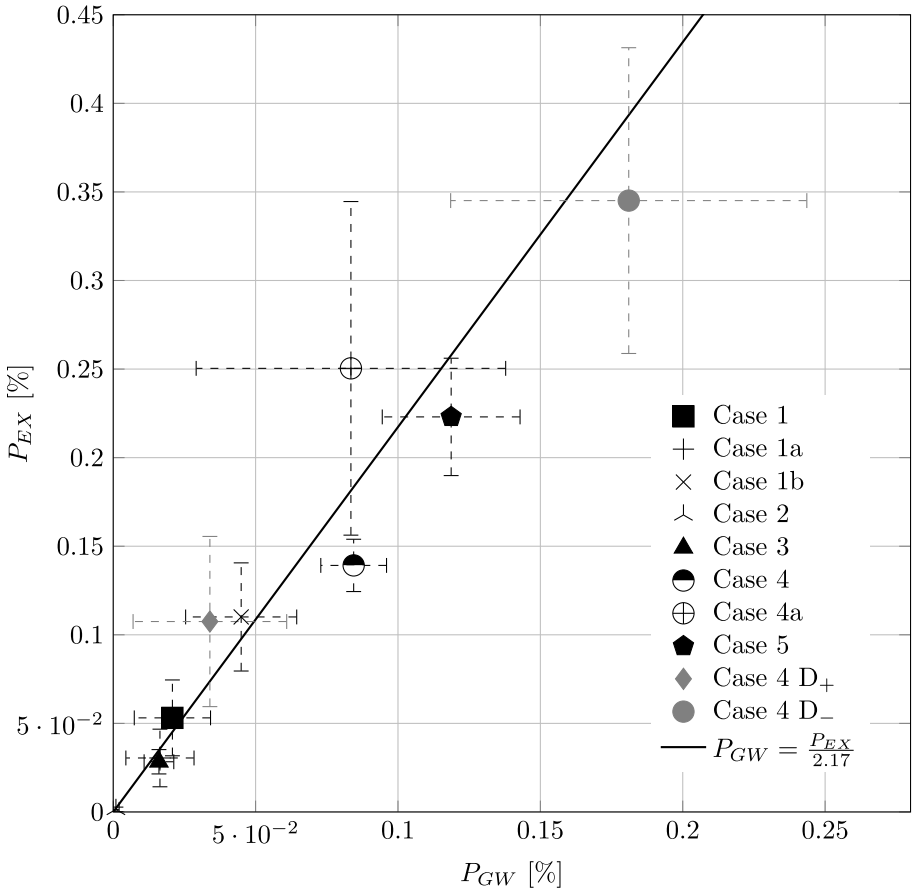

Fig. 17. Relation between P_{GW} and P_{EX} with identified linear relation shown. Dashed lines indicate 95% confidence interval.

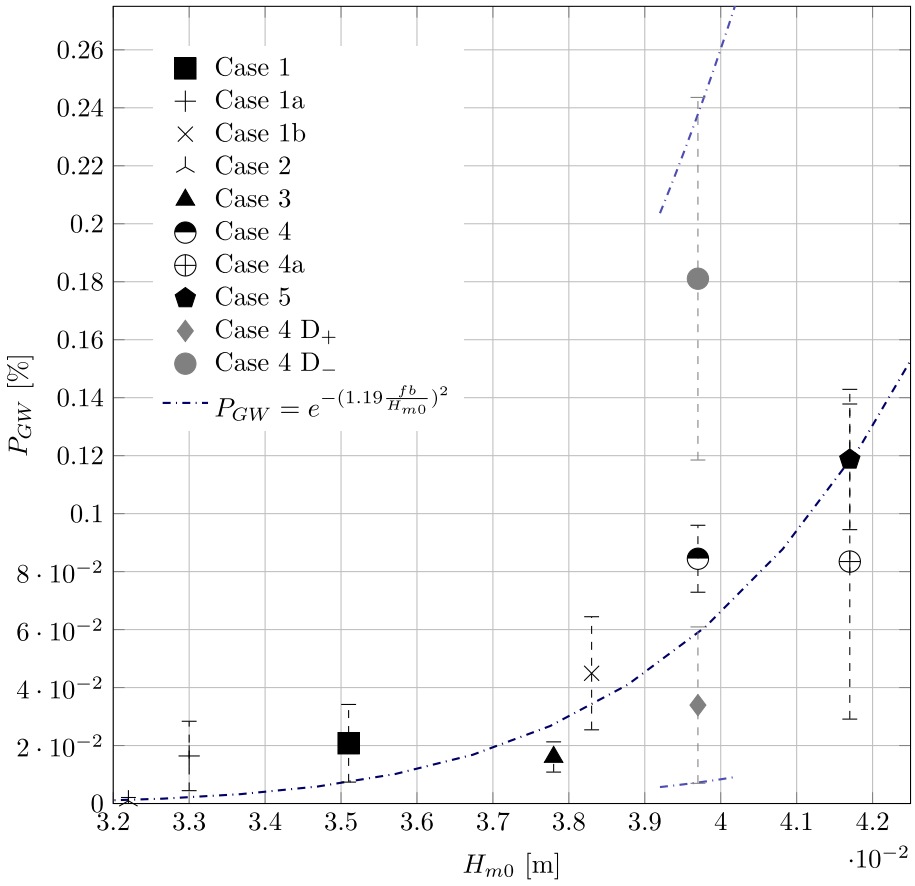

Fig. 18. P_{GW} as a function of H_{m0} shown for all cases, as well as the fitted relation based on Koosheh et al. (2021) (dash-dotted). Grey indicates different drafts and shorter lines of fit are the fits for those different drafts. Dashed lines indicate 95% confidence interval.

A linear relation between P_{EX} and P_{GW} is fitted for, quantified with $P_{GW} = \frac{P_{EX}}{2.17}$. The relation holds for the different wave spectra, forward speeds and drafts tested. The deviations from the relation like case 4 show that the relation does not capture the intricacy of the different physics for exceedance and green water events or the influencing factors.

3.3.2. Relation between P_{GW} and H_{m0}

Finding a relation between P_{GW} and parameters from the environmental conditions would simplify solving Eq. (3) from an engineering perspective. P_{GW} depends on the wave spectrum, draft and forward speed (Table 2). P_{GW} of all tested cases is visualized for various significant wave heights in Fig. 18.

A correlation between H_{m0} and P_{GW} is found. To quantify the correlation, we use work by Koosheh et al. (2021), Franco et al. (1995) and HR Wallingford Ltd (1999), showing a correlation for the probability of wave overtopping for coastal structures. Their formulation includes the relative freeboard crest distance in coastal context and H_{m0}. The relative freeboard crest distance can be translated to the freeboard when considering a ship and the probability of overtopping to the probability of green water. Implementing the translations creates:

$$P_{GW} = e^{-(C\frac{fb}{H_{m0}})^2} = e^{-(1.19\frac{fb}{H_{m0}})^2}, \tag{4}$$

with fb being the still water freeboard at the bow and C a parameter to be fitted for. The relation including the freeboard is in line with Greco (2001) and Hamoudi and Varyani (1998) who showed that the freeboard has the largest influence on green water. The form of the relation is also in line with equations found for the probability of deck wetness based on the Rayleigh distribution (Price and Bishop, 1974; Ogawa, 2003).

With the least-squares method fitting the relation to H_{m0} and P_{GW} for cases with $fb = 0.091$ m C is found to be 1.19, in line with previous research which found values between 1.098 and 1.4 (Franco et al., 1995; HR Wallingford Ltd, 1999; Koosheh et al., 2021). The fit is also visualized in Fig. 18, as well as the fit for the different drafts, with $fb = 0.103$ m and $fb = 0.082$ m, shown for the relevant range of H_{m0}. Overall the fit represents the data.

Forward speed is not included in the relation. In the present study a decrease in forward speed from 0.28 m/s to 0.21 m/s for cases 1a ($V = 0.28$ m/s), 1b ($V = 0.21$ m/s) and 1c ($V = 0.28$ m/s) is found to coincide with an increase in P_{GW}. The relation is not consistent as P_{GW} does not always increase when the ship's forward speed decreases. For case 4a ($V = 0.21$ m/s) a similar P_{GW} was found as for case 4 ($V = 0.25$ m/s). For case 1 ($V = 0.25$ m/s) and case 1a ($V = 0.28$ m/s) also similar P_{GW} were found. The differences in P_{GW} for cases 1a, 1b and 1c are best explained by differences in the wave spectra, as discussed in 2.3. A relation with forward speed could thus not be demonstrated with our present data. Future studies will require increased emphasis on forward speed to allow for a relational formulation of P_{GW} with H_{m0}, fb and V.

3.3.3. Comparing the two estimation methods for P_{GW}

In paragraph 3.3.1 and 3.3.2 two methods are proposed for estimating P_{GW}: one based on P_{EX} and one based on H_{m0}. The methods are compared based on the error between the actual and estimated P_{GW} in Table 5.

The method based on P_{EX} performs better than the method based on H_{m0}. However, the results of the method based on P_{EX} depend on how well P_{EX} is estimated. The values shown in Table 5 are based on the true value of P_{EX} and the relation is also fitted for, thus resulting in the most optimal results. The estimation method for P_{GW} based on H_{m0}

Table 5
Comparing the methods for estimating P_{GW} proposed in the previous paragraphs.

	Experiments	$P_{GW} = \frac{P_{EX}}{2.17}$		$P_{GW} = e^{-(1.19\frac{f_b}{H_{m0}})^2}$	
	P_{GW}	P_{GW}	Error [%]	P_{GW}	Error [%]
1	0.00021	0.00026	23	0.00034	62
1a	0.00016	0.00015	−7.8	0.00017	4.4
1b	0.00045	0.00052	15	0.00121	169
1c	0	0.00002	–	0	–
2	0.00001	0.00001	38	0.00007	686
3	0.00016	0.00014	−13	0.00101	530
4	0.00084	0.00044	−48	0.00193	128
4a	0.00083	0.00087	2.4	0.00346	306
5	0.00119	0.00104	−12	0.00346	191
4 D_+	0.00034	0.00036	7.5	0.00899	2547
4 D_-	0.00181	0.00086	−53	0.00053	−71

uses a few input parameters which will be known when engineering a vessel, making it a practical method, but errors are larger than those of the method based on P_{EX}.

4. Conclusions

A method is proposed to quantify the probability of green water and the expected pressures following a green water event during a ship's operation by finding their distributions. By conducting experiments in a wave–current tank a large green water data set representing 1945 hours of continuous sailing at full scale is obtained. In the experiments the wave spectrum, forward speed and draft were varied.

The distribution of the maximum pressures is identified as the Fréchet distribution, an extreme value distribution. A difference in skew between the theoretical distribution and the data indicates that the Fréchet distribution gives conservative estimations for large pressures. The time between the occurrence of green water is exponentially distributed for all different tested cases, indicating that when a green water event occurs is independent of the time since the last event. The same is true for deck exceedance events.

An equation is formulated to calculate the probability of a limit pressure being exceeded during a ship's operation. The sailing time, probability of green water and parameters of the Fréchet distribution for maximum pressures are taken as input.

Two methods to calculate the probability of green water occurring are presented. The first method uses the linear relation between the probability of deck exceedance and the probability of green water. The second method calculates the probability of green water occurrence based on the freeboard and significant wave height. The first method gives estimations that are closer to the experimental data while the second is more practical from an engineering perspective.

CRediT authorship contribution statement

A.D. Boon: Conceptualization, Methodology, Formal analysis, Investigation, Resources, Data curation, Visualization, Writing – original draft. **P.R. Wellens:** Conceptualization, Writing – review and editing, Supervision.

Declaration of competing interest

The authors declare that they have no known competing financial interests or personal relationships that could have appeared to influence the work reported in this paper.

Data availability

The data is available through Wellens and Boon (2022).

Acknowledgements

Special thanks to C.P. Poot, F.J. Sterk, J.G. den Ouden, P. Taudin Chabot, J. Rodrigues Montiero and J. van Driel for all the help with the test facility and experiments. Thanks to A. Derumigny for making the time to discuss statistics. This publication is part of the project "Multi-fidelity Probabilistic Design Framework for Complex Marine Structures, The Netherlands" (project number TWM.BL.019.007) of the research programme "Topsector Water & Maritime: the Blue route", which is (partly) financed by the Dutch Research Council (NWO) and Stichting Bijlboegfonds, The Netherlands.

Appendix A. Uncertainty analysis

All measurements are subject to some measurement error. To find the effect of the results an uncertainty analysis has been conducted. Errors are assumed to be independent, normally distributed and not biased. The measurement error has been minimized for all distance, weight and current velocity measurements by repeating measurements at least three times and using the average. The measurement error is estimated to be ±0.001 m for the distances, ±0.001 kg for the weights and ±0.005 m/s for velocities. The measurements for the natural frequency were also obtained by taking the average of repeated excitation tests. The estimated uncertainty introduced by the frequency resolution of the used Fourier transform is ±0.005 Hz. The error in testing duration is estimated to be ±5 s. Besides measurement errors there is also a possibility that a green water or exceedance event was misidentified, leading to an estimated error in the number of events of ±1.0%. The wave probe, RWE probe and pressure sensors were calibrated and thus the variation has been measured. No errors above respectively 2.4%, 1.5% and 3% as percentages of the range were found. These maximum errors were found near the extremities of the sensor ranges. The maximum estimated percentage values of all the measurement errors are given in Table A.6. The errors are the errors as a percentage of the properties of the experiment (see Table 1).

The propagation of the measurement errors on the results of the following calculations is analysed. The error for the radius of gyration is 0.8% caused by the propagation of the weight and distance measurement errors. The waves in the tank were measured with a wave probe with the same relative velocity to the waves as the ship model, thus measuring the wave encounter frequency. To calculate T_p V has to be accounted for, which has an estimated uncertainty of ±0.005 m/s, propagating to an uncertainty of ±0.3% for T_p.

The measurement errors also propagate to probabilities and maximum pressures, causing the uncertainties shown in Table A.7. The uncertainty in P_{GW} and P_{EX} is caused by the errors in testing duration and identified events. The uncertainties of λ_{GW} and λ_{EX} are equal to the uncertainties of P_{GW} and P_{EX}. The measurement error in the pressures is 3%, causing an uncertainty of 3% for $p_{deck,max}$ and $p_{box,max}$. For $P_{deck,max}$ and $P_{box,max}$ an average over a set of sensors was used, and as the errors are assumed to be independent, normally distributed

Table A.6
Maximum estimated measurement errors.

Measurement	Error as % of used value
Length between perpendiculars	±0.3%
Breadth moulded	±1.5%
Depth moulded	±2.4%
Draft	±4.8%
Total mass	±0.2%
Natural heave frequency	±0.5%
Natural pitch frequency	±0.3%
Deck box (L × W × H)	±0.7 × 0.6 × 1.1%
Distance to deck box from stem	±0.3%
Location RWE probe from stem	±2.5%
Vertical centre of gravity	±0.6%
Longitudinal centre of gravity	±0.1%
Forward velocity	±2.4%
Testing time	±0.1%
Number of events	±1.0%
Wave height	±2.4%
RWE	±1.5%
Pressures	±3.0%

Table A.7
Maximum uncertainties for pressures and probabilities caused by the propagation of errors.

Case	P_{GW} & P_{EX}	$\overline{P}_{max}$	$\overline{p}_{max}$
1	±2.0%	±0.4%	±0.8%
1a	±2.0%	±0.4%	±0.9%
1b	±2.0%	±0.2%	±0.5%
1c	–	–	–
2	±2.0%	±1.1%	±2.1%
3	±2.0%	±0.2%	±0.4%
4	±2.0%	±0.1%	±0.2%
4a	±2.2%	±0.4%	±0.8%
5	±2.0%	±0.1%	±0.2%
4 D_+	±2.1%	±0.5%	±0.9%
4 D_-	±2.1%	±0.2%	±0.4%

and not biased the error reduces with $\frac{1}{\sqrt{2(N-1)}}$ (Grabe, 2005), with N equal to the number of sensors (three useable deck sensors and three deck box sensors), leading to an error of 1.5% for $P_{deck,max}$ and $P_{box,max}$. The pressure error also propagates to the parameters of the Fréchet distribution. For the fitting of the distribution, the pressures are analysed as a set so the uncertainties of the mean of the impact pressures per case will decrease with $\frac{1}{\sqrt{2(N-1)}}$, with N this time as the number of events included in the calculation. The resulting uncertainty of the mean impact pressures per case ($\overline{P}_{max}$ and $\overline{p}_{max}$) is shown in Table A.7. This uncertainty propagates again to the skew of the data. Assuming the same distribution of pressures but a shift in the mean of the pressures equal to the values in Table A.7 the maximum estimated error in the skew is ±0.6%.

References

Abdussamie, Nagi, Drobyshevski, Yuriy, Ojeda, Roberto, Thomas, Giles, Amin, Walid, 2017. Experimental investigation of wave-in-deck impact events on a TLP model. Ocean Eng. 142, 541–562. http://dx.doi.org/10.1016/J.OCEANENG.2017.07.037.

Ariyarathne, Kusalika, Chang, Kuang An, Mercier, Richard, 2012. Green water impact pressure on a three-dimensional model structure. Exp. Fluids (ISSN: 07234864) 53 (6), 1879–1894. http://dx.doi.org/10.1007/s00348-012-1399-9, URL https://link.springer.com/article/10.1007/s00348-012-1399-9.

Berhault, C., Guerin, P., 1998. Experimental and numerical investigations on the green water effects on FPSOs. In: Proceedings of the Eighth. URL http://onepetro.org/ISOPEIOPEC/proceedings-pdf/ISOPE98/All-ISOPE98/ISOPE-I-98-043/1933373/isope-i-98-043.pdf/1.

Buchner, B., 2002. Green Water on Ship-Type Offshore Structures (Ph.D. thesis). Technische Universiteit Delft, URL https://repository.tudelft.nl/islandora/object/uuid%3Af0c0bd67-d52a-4b79-8451-1279629a5b80.

Cox, Daniel T., Scott, Christopher P., 2001. Exceedance probability for wave overtopping on a fixed deck. Ocean Eng. (ISSN: 00298018) 28 (6), 707–721. http://dx.doi.org/10.1016/S0029-8018(00)00022-6.

Cuomo, Giovanni, Allsop, William, Bruce, Tom, Pearson, Jonathan, 2010. Breaking wave loads at vertical seawalls and breakwaters. Coast. Eng. (ISSN: 03783839) 57 (4), 424–439. http://dx.doi.org/10.1016/J.COASTALENG.2009.11.005.

de Haan, Laurens, Ferreira, Ana, 2000. Extreme Value Theory: An Introduction. Springer, Lisbon, URL https://link-springer-com.tudelft.idm.oclc.org/content/pdf/10.1007%2F0-387-34471-3.pdf.

Faltinsen, O.M., Greco, M., Landrini, M., 2002. Green water loading on a FPSO. J. Offshore Mech. Arct. Eng. (ISSN: 08927219) 124 (2), 97–103. http://dx.doi.org/10.1115/1.1464128.

Federation of American Scientists, 1999. LPD 4 Austin class - Navy ships. URL https://man.fas.org/dod-101/sys/ship/lpd-4.htm.

Fonseca, Nuno, Guedes Soares, C., 2005. Experimental investigation of the shipping of water on the bow of a containership. J. Offshore Mech. Arct. Eng. (ISSN: 0892-7219) 127 (4), 322–330. http://dx.doi.org/10.1115/1.2087527, URL https://asmedigitalcollection.asme.org/offshoremechanics/article/127/4/322/446825/Experimental-Investigation-of-the-Shipping-of.

Franco, L., de Gerloni, M., van der Meer, J.W., 1995. Wave overtopping on vertical and composite breakwaters. Proc. Coastal Eng. Conf. (ISSN: 08938717) 1, 1030–1044. http://dx.doi.org/10.1061/9780784400890.076.

Grabe, Micheal, 2005. Measurement Uncertainties in Science and Technology. Springer Berlin Heidelberg, New York, ISBN: 3-540-20944-1.

Greco, Marilena, 2001. A Two-Dimensional Study of Green-Water Loading. (Ph.D. thesis). Norwegian University of Science and Technology.

Greco, M., Colicchio, G., Faltinsen, O.M., 2007. Shipping of water on a two-dimensional structure. Part 2. J. Fluid Mech. (ISSN: 00221120) 581, 309–332. http://dx.doi.org/10.1017/S0022112004002691.

Guedes Soares, C., Pascoal, R., 2005. Experimental study of the probability distributions of green water on the bow of floating production platforms. J. Offshore Mech. Arct. Eng. (ISSN: 08927219) 127 (3), 234–242. http://dx.doi.org/10.1115/1.1951773.

Guerriero, Vincenzo, 2012. Power law distribution: Method of multi-scale inferential statistics. J. Mod. Math. Front. 1 (1), 21–28.

Hamoudi, B., Varyani, K.S., 1998. Significant load and green water on deck of offshore units/vessels. Ocean Eng. 25 (8), 715–731.

Hattori, Masataro, Arami, Atsushi, Yui, Takamasa, 1994. Wave impact pressure on vertical walls under breaking waves of various types. Coast. Eng. (ISSN: 03783839) 22, 79–114. http://dx.doi.org/10.1016/0378-3839(94)90049-3.

Hernández-Fontes, Jassiel V., Hernández, Irving D., Mendoza, Edgar, Silva, Rodolfo, 2020a. Green water evolution on a fixed structure induced by incoming wave trains. Mech. Based Des. Struct. Mach. (ISSN: 15397742) http://dx.doi.org/10.1080/15397734.2020.1791179.

Hernández-Fontes, Jassiel V., Hernández, Irving D., Mendoza, Edgar, Silva, Rodolfo, da Silva, Eliana Brandão, de Sousa, Matheus Rocha, Gonzaga, José, Kamezaki, Raíssa S.F., Torres, Lizeth, Esperança, Paulo T.T., 2021. On the evolution of different types of green water events. Water (ISSN: 2073-4441) 13 (9), http://dx.doi.org/10.3390/W13091148, URL https://www.mdpi.com/2073-4441/13/9/1148/htm, https://www.mdpi.com/2073-4441/13/9/1148.

Hernández-Fontes, Jassiel V., Vitola, Marcelo A., Esperança, Paulo T.T., Sphaier, Sergio H., Silva, Rodolfo, 2020b. Patterns and vertical loads in water shipping in systematic wet dam-break experiments. Ocean Eng. (ISSN: 00298018) 197, http://dx.doi.org/10.1016/j.oceaneng.2019.106891.

HR Wallingford Ltd, 1999. Wave Overtopping of Seawalls Design and Assessment Manual. Technical report, Environment Agency.

Kirkgoz, M. Salih, 1990. An experimental investigation of a vertical wall response to breaking wave impact. Ocean Eng. 17 (4), 379–391.

Koosheh, Ali, Etemad-Shahidi, Amir, Cartwright, Nick, Tomlinson, Rodger, van Gent, Marcel R.A., 2021. Individual wave overtopping at coastal structures: A critical review and the existing challenges. Appl. Ocean Res. (ISSN: 01411187) 106, http://dx.doi.org/10.1016/J.APOR.2020.102476.

Lee, Gang Nam, Jung, Kwang Hyo, Malenica, Sime, Chung, Yun Suk, Suh, Sung Bu, Kim, Mun Sung, Choi, Yong Ho, 2020. Experimental study on flow kinematics and pressure distribution of green water on a rectangular structure. Ocean Eng. (ISSN: 00298018) 195, http://dx.doi.org/10.1016/j.oceaneng.2019.106649.

Lee, Hyun Ho, Lim, Ho Jeong, Rhee, Shin Hyung, 2012. Experimental investigation of green water on deck for a CFD validation database. Ocean Eng. (ISSN: 00298018) 42, 47–60. http://dx.doi.org/10.1016/j.oceaneng.2011.12.026.

Lowell, Stephanie, Irani, Rishad A., 2020. Sensitivity analysis of plunger-type wavemakers with water current. In: Global Oceans 2020: Singapore – US Gulf Coast. ISBN: 9781728154466, pp. 1–9. http://dx.doi.org/10.1109/IEEECONF38699.2020.9389447.

Massey, Frank J., 1951. The Kolmogorov–Smirnov test for goodness of fit. J. Amer. Statist. Assoc. 46 (253), 68–78.

Mori, Nobuhito, Cox, Daniel T., 2003. Dynamic properties of green water event in the overtopping of extreme waves on a fixed dock. Ocean Eng. (ISSN: 00298018) 30 (16), 2021–2052. http://dx.doi.org/10.1016/S0029-8018(03)00073-8.

Ogawa, Yoshitaka, 2003. Long-term prediction method for the green water load and volume for an assessment of the load line. J. Mar. Sci. Technol. (ISSN: 09484280) 7 (3), 137–144. http://dx.doi.org/10.1007/s007730300004, URL https://link-springer-com.tudelft.idm.oclc.org/article/10.1007/s007730300004.

Peregrine, D.H., 2003. Water-wave impact on walls. Annu. Rev. Fluid Mech. (ISSN: 00664189) 35, 23–43. http://dx.doi.org/10.1146/annurev.fluid.35.101101.161153.

Price, W.G., Bishop, Richard Evelyn Donohue, 1974. Probabilistic Theory of Ship Dynamics. Chapman and Hall, London, ISBN: 0470697334.

Ross, Sheldon M., 2020. Confidence interval of the mean of the exponential distribution. In: In Introduction to Probability and Statistics for Engineers and Scientists, Chapter 7, sixth ed. Elsevier Academic Press, ISBN: 9780128177471, pp. 267–282.

Ruggeri, Felipe, Watai, Rafael A., de Mello, Pedro Cardozo, Sampaio, Claudio Mueller P., Simos, Alexandre N., de Carvalho e. Silva, Daniel Fonseca, 2015. Fundamental green water study for head, beam and quartering seas for a simplified FPSO geosim using a mixed experimental and numerical approach. Mar. Syst. Ocean Technol. (ISSN: 21994749) 10 (2), 71–90. http://dx.doi.org/10.1007/S40868-015-0007-2/FIGURES/46, URL https://link-springer-com.tudelft.idm.oclc.org/article/10.1007/s40868-015-0007-2.

Song, Youn Kyung, Chang, Kuang An, Ariyarathne, Kusalika, Mercier, Richard, 2015. Surface velocity and impact pressure of green water flow on a fixed model structure in a large wave basin. Ocean Eng. (ISSN: 00298018) 104, 40–51. http://dx.doi.org/10.1016/j.oceaneng.2015.04.085.

Wellens, P.R., Boon, A.D., 2022. Data from long-running green water experiments in various sea states at model scale (Repository). 4TU.ResearchData, URL https://doi.org/10.4121/21031981.

Wilk, M.B., Gnanadesikan, R., 1968. Probability plotting methods for the analysis of data. Biometrika 55 (1), 1, URL http://biomet.oxfordjournals.org/.